JOURNAL OF GEOPHYSICAL RESEARCH, VOL. 104, NO. C11, PAGES 25,697–25,705, NOVEMBER 15, 1999

A new interpretation of multifrequency/multipolarization radar signatures of the Gulf Stream front

Susanne Ufermann[1] and Roland Romeiser

Institute of Oceanography, University of Hamburg, Hamburg, Germany

Abstract. Radar signatures which are observed on SIR-C/X-SAR multifrequency/multipolarization synthetic aperture radar images of the Gulf Stream off the U.S. east coast are compared with results of simulations with a numerical radar imaging model. Based on in situ data, current and wind variations are included into the model as well as a variation of the thermal stability of the marine atmospheric boundary layer across the Gulf Stream front. According to our model predictions, all of these parameter variations can cause radar signatures of similar shape and modulation depth. But, due to specific dependencies of radar signatures on variations of surface currents and winds, we show that it is possible to distinguish between radar signatures of oceanic and atmospheric origin in multifrequency/multipolarization images and to estimate the corresponding current and wind variations independently. For one set of radar images we derive a most likely scenario of oceanic and atmospheric parameters during the time of the image acquisition for which good overall agreement between observed and simulated radar signatures is obtained at most radar channels.

1. Introduction

The Gulf Stream as one of the biggest jets in the world ocean plays an important role for climate conditions of the Northern Hemisphere and the oceanic circulation system. As a part of the Gulf Stream system which extends from the Gulf of Mexico to northern Europe, the Gulf Stream itself is situated between the Strait of Florida and the Newfoundland Rise in the North Atlantic Ocean. At a latitude of ~35°N, it leaves the U.S. coast and continues as free jet into the Atlantic Ocean. In these regions, mass transports of 70-100 Sv (1 Sv (sverdrup) = $1\times10^6\,\mathrm{m^3s^{-1}}$) and a heat transport of 10^{15} W can be reached [*Rossby,* 1991; *Tomczak and Godfrey,* 1994]. Current speeds can exceed 1.5 $\mathrm{m\,s^{-1}}$, and temperature differences of up to 15°C between the Gulf Stream waters and the adjacent slope waters of the North American shelf are found at the northwestern edge of the Gulf Stream.

Radar images like the images in Figure 1, which show this region of the Gulf Stream, often exhibit an elongated signature that extends from the southwest toward the northeast. This direction is also well known as the main flow direction of the Gulf Stream where it leaves the U.S. coast. It was shown in recent publications that the observed radar signatures actually correspond to the Gulf Stream front, although it does not seem to be clear which parameter variations predominantly cause the radar signatures: While some authors mainly assign the signatures to a variation of the sea surface temperature [e.g., *Mango et al.,* 1995; *Beal et al.,* 1997], signatures are explained by current or wind variations in other publications [*Valenzuela et al.,* 1991, 1994; *Marmorino et al.,* 1994; *Askari et al.,* 1997]. Since both explanations do not seem to account for the variety of observed radar signatures, we carry out an analysis which is not confined to the investigation of the influence of only one of the possible atmospheric and oceanic mechanisms on radar signatures but which accounts for the effect of current variation, wind, and atmospheric stability at the same time.

In general, radar signatures of oceanic fronts must result from physical mechanisms which modulate the sea surface roughness. Three main mechanisms which come to mind are (1) modulation of the surface wave spectrum by hydrodynamic wave-current interaction, (2) variation of the wind-induced part of the surface wave spectrum with the stratification of the marine atmospheric boundary layer (MABL), as determined by the air-sea temperature differences at both sides of the front, and (3) damping of short surface waves in the presence of surface films accumulated by convergent currents. Despite different physical sources, all three

[1]Now at Southampton Oceanography Centre, Southampton, United Kingdom.

Paper number 1999JC900237.
0148-0227/99/1999JC900237$09.00

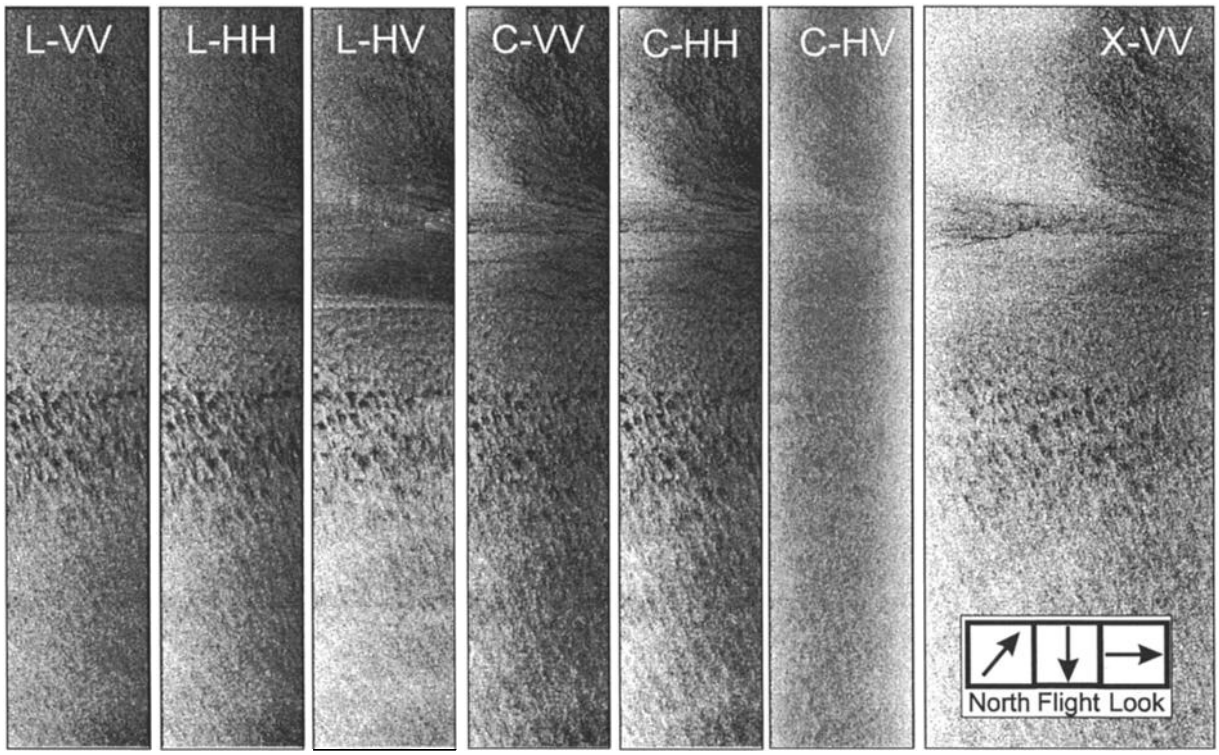

Figure 1. Multifrequency/multipolarization SAR images of the same scene of the northwestern edge of the Gulf Stream. The images were acquired from the space shuttle on April 17, 1994, 1622 UTC at an incidence angle of 31° (at the image center). The imaged area at L and C band is 20 km × 100 km and at X band 40 km × 100 km.

modulation mechanisms can produce similar radar signatures, which allows a variety of possible interpretations of single radar images if no additional information is available. However, it is well known that variations in the wind field on relatively short scales in space or time will mainly modulate short surface waves (wavelengths of centimeters to decimeters), which act as resonant Bragg waves for microwave radars, while hydrodynamic modulation will have a stronger effect on longer waves (wavelengths of decimeters to meters). This behavior results in different dependencies of radar signatures of oceanic and atmospheric origin on radar frequency and polarization [*Romeiser,* 1997]. We will show in the following that owing to this fact, current- and wind-induced contributions to radar signatures of oceanic fronts can be identified where multifrequency/multipolarization radar data are available.

In section 2, radar and in situ data from the Gulf Stream edge are presented that are used for our study. Section 3 explains the theoretical background of the simulations of radar signatures at the Gulf Stream front that we have carried out and gives a short description of the proposed radar imaging model; a comparison of observed and simulated radar signatures is presented in section 4. In section 5 the results of our investigations are discussed, and section 6 summarizes our main conclusions.

2. Data From the Gulf Stream Edge

2.1. Radar Images

On April 17, 1994, 1622 UTC, a set of multifrequency/multipolarization radar images of the Gulf Stream front off the east coast of the United States was acquired within the framework of the Spaceborne Imaging Radar-C/X-Band Synthetic Aperture Radar (SIR-C/X-SAR) mission [*Jordan et al.,* 1995; *Zink and Bamler,* 1995]. Two synthetic aperture radar (SAR) sensors (SIR-C, operating at L and C band, and X-SAR, operating at X band) were mounted aboard the U.S. space shuttle Endeavour during this 10-day mission to acquire two-dimensional high-resolution multifrequency/multipolarization radar images of the Earth's surface under various incidence angles.

The SIR-C/X-SAR images used in this investigation which are shown in Figure 1, were acquired at L (1.25 GHz) and C band (5.30 GHz), VV, HH, and HV polarization, and at X band (9.60 GHz), VV polarization; the incidence angle at the center of the L and C band images (36.64°N, 73.61°W) was 31°. Owing to the low signal-to-noise ratio (SNR) of the image acquired at C band, HV polarization, this image is not well suited for our quantitative analysis.

Figure 2 shows a section of the SIR-C/X-SAR image acquired at L band, HV polarization. The upper part

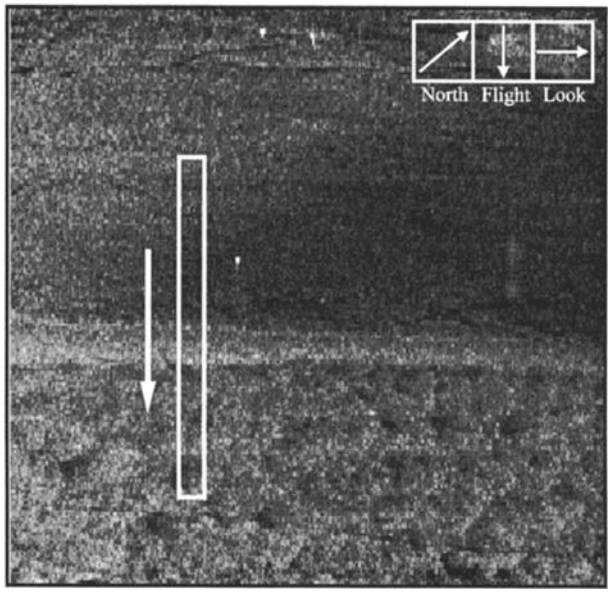

Figure 2. Section from the SIR-C/X-SAR image of the Gulf Stream front at L band, HV polarization, shown in Figure 1. The imaged area is approximately 15 km × 15 km. The white rectangle marks the area for which intensity profiles are shown in Figure 5.

of this image shows a region outside the Gulf Stream, whereas the lower part, characterized by a mottled pattern, shows a region inside the Gulf Stream. Such mottled patterns are often observed in radar images of regions where a negative air-sea temperature difference results in unstable thermal stratification of the MABL, leading to a formation of atmospheric convective cells [*Mitnik,* 1992; *Alpers,* 1995; *Ufermann et al.,* 1998]. We will show in the following that indeed, the thermal stratification over the Gulf Stream was unstable at the time of the shuttle overflight. An explicit discussion of the atmospherically induced radar signatures over the Gulf Stream is given by *Ufermann and Romeiser* [this issue].

This study concentrates on the radar signature of the Gulf Stream front which is characterized by significant variations of the normalized radar backscattering cross section (NRCS) in all radar channels within a narrow band extending over the whole swath width. In previous studies based on the data set used for our investigations [*Askari et al.,* 1997; *Chubb et al.,* 1999], this radar signature has been attributed to the effect of a strong current shear at the thermal front.

2.2. In Situ Data

During the shuttle overflight, in situ data were collected in the region of the Gulf Stream front by scientists from the Naval Research Laboratory (NRL) aboard the R/V *Cape Hatteras.* At the time of the image acquisition, data from these measurements indicate a mean wind speed of 3.5 $\mathrm{m\,s^{-1}}$, blowing from 130°N, which corresponds to a direction almost perpendicular to the front, coming from the region inside the Gulf Stream. *Askari et al.* [1997] and *Chubb et al.* [1999] specified the surface currents to be 0.8 $\mathrm{m\,s^{-1}}$ outside and 1.5 $\mathrm{m\,s^{-1}}$ inside the Gulf Stream, directed toward the northeast (right-hand side of the images in Figure 1). In this context, one should note that although the change in the surface current at the Gulf Stream front is undoubtedly dominated by a current shear, the accuracy of the available current data also justifies consideration of the effect of possible small current components normal to the front in our numerical simulations. Furthermore, the in situ data exhibit a change of the thermal stability of the MABL across the front from $T_{\mathrm{air}} - T_{\mathrm{sea}} = +2.0°\mathrm{C}$ (stable) outside the Gulf Stream to $T_{\mathrm{air}} - T_{\mathrm{sea}} = -7.5°\mathrm{C}$ (unstable) inside the Gulf Stream.

3. Theory

In order to interpret radar images of oceanic and atmospheric phenomena, it is necessary to understand the different impact that both kinds of phenomena can have on the sea surface roughness which determines a radar signature and to understand how atmospheric and oceanic phenomena interact with each other. For the investigations of this work we have carried out simulations with the numerical radar imaging model of the University of Hamburg [*Romeiser and Alpers,* 1997; *Romeiser et al.,* 1997] for a variety of current, wind, and MABL stratification conditions. The wave module of our model is based on weak hydrodynamic interaction theory and has been implemented such that it can handle independently defined current and wind fields as input. In the integration of the action balance equation, as described by *Romeiser and Alpers* [1997], a spatially varying surface current determines integration paths in five-dimensional wavenumber-space-time space; the source function varies with the equilibrium wave spectrum and relaxation rate, which both depend on the local wind vector. In this way, current and wind variations enter into the calculations in a physically consistent way and at the same time. As mentioned in section 1, spatial variations in the surface wind will mainly act on short waves, while hydrodynamic wave-current interaction will have the strongest effect at wavelengths of decimeters to meters [*Romeiser,* 1997; *Romeiser and Alpers,* 1997]. Note that this is a fundamental result of the theory, which does not depend very much on the parameterizations of the equilibrium wave spectrum or the relaxation rate. Standard parameterizations in our model are the ones proposed by *Romeiser et al.* [1997] and by *Romeiser and Alpers* [1997], respectively.

Our wave model generates a complete two-dimensional modulated wave spectrum for each grid point, which then enters into a composite surface scattering model for the calculation of NRCS arrays, i.e., simulated radar images. The composite surface model is based on Bragg scattering theory [*Wright,* 1968; *Valenzuela,* 1978] and accounts for contributions of the whole two-dimensional surface wave spectrum to the NRCS. These contribu-

tions are represented by terms of zeroth and second order in the surface slopes of waves which are long compared to the Bragg waves that are in resonance with the radar signal. All terms are proportional to the intensity of the Bragg waves, while the second-order terms are also proportional to the mean square surface slopes parallel and normal to the radar look direction. The relative contribution of the second-order terms to the NRCS depends on the polarization of the radar in such a way that intensity variations of longer waves have a stronger impact on radar signatures at HH than on those at VV polarization. The strongest effect of longer waves is obtained at HV or VH (i.e., cross) polarization, where the zeroth-order terms of the NRCS vanish.

For the simulation of the surface current and wind variation in this study we have parameterized the current and wind fields in a simple way: Surface current gradients as well as wind speed gradients are decomposed into gradients of a current/wind component normal to the front, U_x and u_x, respectively, and another component parallel to the front, U_y and u_y. On the basis of an expression also used by *Askari et al.* [1997], the current field is modeled by

$$(U_x, U_y) = \boldsymbol{U}(x) = \boldsymbol{U_0} + \left[\frac{\boldsymbol{\delta U}}{2} \tanh \left(\frac{x - x_c}{\delta x_c} \right) \right] \quad (1)$$

where $\boldsymbol{U_0}$ and $\boldsymbol{\delta U}$ are constants denoting the mean current speed and the current speed variation, respectively. Furthermore, x_c determines the location of the current front on the x axis, while the width over which the current variation extends is represented by δx_c.

Using the same approach, we model the wind field by

$$(u_x, u_y) = \boldsymbol{u}(x) = \boldsymbol{u_0} + \left[\frac{\boldsymbol{\delta u}}{2} \tanh \left(\frac{x - x_w}{\delta x_w} \right) \right] \quad (2)$$

In this case, $\boldsymbol{u_0}$ and $\boldsymbol{\delta u}$ represent the mean wind speed at a height of 10 m and the wind speed variation, respectively; x_w determines the location of the wind front on the x axis while the width over which the wind variation extends is represented by δx_w. As we will explain in the following, a superposition of two wind variations of form (2) will be used in our final simulations in order to account for explicit variations of the wind vector $\boldsymbol{u}$ (outside the Gulf Stream) and for variations of the wind stress with the thermal stratification in the MABL (at the Gulf Stream front) which are also parameterized as variations of $\boldsymbol{u}$.

The atmospheric buoyancy and arising turbulence associated with unstable stratification can lead to an increase of the NRCS of the ocean surface with respect to a stable scenario at the same nominal wind speed. In previous studies [*Keller et al.*, 1989; *Beal et al.*, 1997] it was found that an inversion of the atmospheric stratification can result in an increase of the NRCS by several decibels where MABL stratification changes are as pronounced as in the vicinity of the Gulf Stream front. Thus both the current gradients and the changing atmospheric stratification at the Gulf Stream front can be expected to affect the radar imagery significantly.

Quantitative information on the influence of atmospheric stability on radar images of the ocean surface and NRCS changes due to stratification effects are presented by *Keller et al.* [1989] and *Wu* [1991]. Figure 3 shows the NRCS versus air-sea temperature difference for a scenario with wind speeds between 6 and 7 $\mathrm{m\,s^{-1}}$ from *Keller et al.* [1989] (open circles) together with the NRCS measured at both sides of the Gulf Stream front under stable and unstable stratification conditions at wind speeds of ~3.5 $\mathrm{m\,s^{-1}}$ (solid circles). Deviations between absolute NRCS levels reported by *Keller et al.* [1989] that were observed from a research platform and NRCS values derived from the SIR-C/X-SAR data can be explained by systematic differences between the experimental conditions: According to our model, NRCS values for C band, VV, should be ~2 dB higher at a wind speed of 3.5 $\mathrm{m\,s^{-1}}$ and an incidence angle of 31° (SIR-C/X-SAR conditions) than at 6.5 $\mathrm{m\,s^{-1}}$ and 45° (*Keller et al.* [1989] conditions). This is in good agreement with the offset found in Figure 3. More important, the trend in the two data points from the Gulf Stream front is in reasonable agreement with the one found in the data of *Keller et al.* [1989]. Therefore it appears to be reasonable to attribute the observed difference of ~1.4 dB between the NRCS of regions inside and outside the Gulf Stream to the effect of the stratification variation of the MABL.

Since the only parameter in our imaging model which represents the effect of the wind field on ocean waves is the wind speed at 10 m height, $\boldsymbol{u}$, the effect of vari-

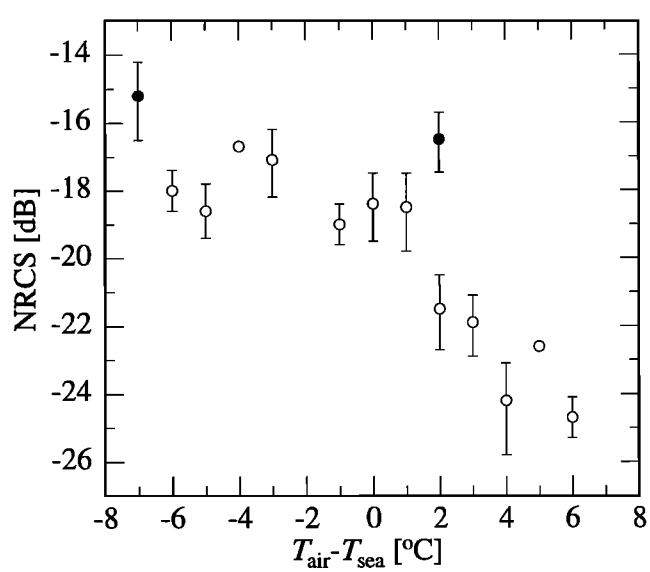

Figure 3. C band (VV polarization) NRCS versus air-sea temperature difference for wind speeds between 6 and 7 $\mathrm{m\,s^{-1}}$ as measured by *Keller et al.* [1989] at the North Sea research platform (open circles) and as observed at the Gulf Stream front (solid circles).

ations of the stratification, which should normally be represented by variations of the friction velocity or the drag coefficient, must be translated into an equivalent modification of u under the assumption of a constant drag coefficient. While this approach may appear questionable from a general point of view, it seems to be adequate as long as we are mainly interested in intensity variations of relatively short surface waves. In general, the "effective wind speed" acting on long and short waves can be quite different, and the differences may vary with the atmospheric stratification.

Figure 4 shows how we have determined a wind speed change at 10 m height that represents the MABL stratification change in our model calculations: We have used our radar imaging model to calculate NRCS values for the incidence angle of 31° and the wind direction of 130°N for varying wind speeds. The lines in Figure 4 indicate that under neutral stratification conditions, the required increase of the NRCS by ~1.4 dB would correspond to an increase of u from 3.5 to 4.8 $\mathrm{m\,s^{-1}}$. These values were used in our simulations to account for the variation of the thermal stratification across the Gulf Stream front.

4. Results

Figure 5a shows the variation of the NRCS across the Gulf Stream front along the line inserted in Figure 2 for all SIR-C/X-SAR radar frequencies and polarizations. All profiles exhibit a dip-like behavior: Before the Gulf Stream front (0-3 km) they show a quasi-constant NRCS level, then a decrease appears in the profiles to a local minimum at the Gulf Stream front (4-5 km) and an increase after the front (6-10 km) up to a level that is, in some cases, even higher than the level before the front. We attribute relatively large variations of the NRCS in this part of the profiles to roughness variations caused by atmospheric convective cells [see *Ufermann and Romeiser*, this issue].

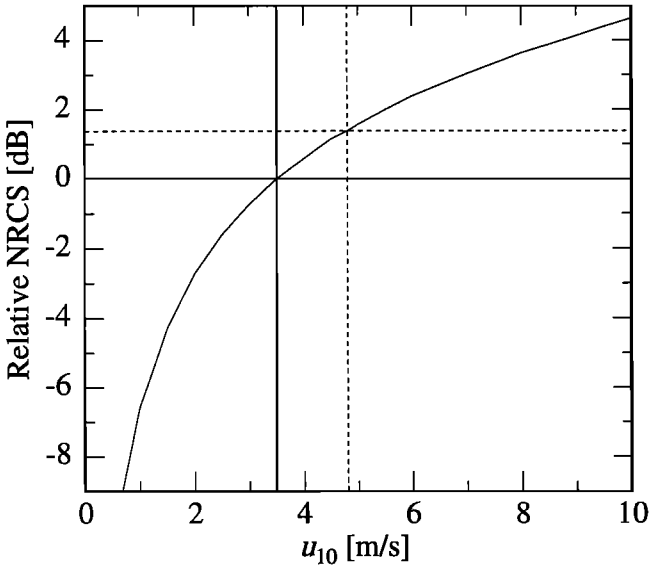

Figure 4. Simulated relative NRCS for different wind speeds for neutral MABL stratification as calculated with our model for C band, VV polarization, under an incidence angle of 31° and a wind direction of 130°N; NRCS values, as observed on both sides of the Gulf Stream front, and corresponding calculated wind speeds are marked: solid line indicates values for the region outside the Gulf Stream; dashed line indicates values for the region inside the Gulf Stream.

4.1. Variation of Oceanic Parameters

As the current shear is the most remarkable feature at the Gulf Stream front, it was expected to have a dominant impact on radar signatures. In order to investigate this hypothesis, theoretical radar signatures for pure surface current gradients were calculated first, assuming a constant wind speed of 3.5 $\mathrm{m\,s^{-1}}$ and no variation in the MABL stratification. Values for the mean current U_{0y} and the current variation δU_y were adopted from *Askari et al.* [1997] to be 1.15 $\mathrm{m\,s^{-1}}$ and 0.70 $\mathrm{m\,s^{-1}}$, respectively; x_c was set to 4500 m. The width of the area over which the current change extends, δx_c, as well as possible small x components of $\boldsymbol{U_0}$ and $\boldsymbol{U}$, forming a convergence or divergence, were optimized iteratively.

Figure 5b shows that the modulation depths of the observed NRCS profiles are strongly underestimated by our model if only a current shear is assumed. A better agreement between observed and simulated radar signatures was obtained after introducing an additional divergence normal to the front ($U_{0x} = 0.4$ $\mathrm{m\,s^{-1}}$, $\delta U_x = 0.4$ $\mathrm{m\,s^{-1}}$), where the width of the observed signatures is best reproduced with $\delta x_c = 800$ m. Currents and simulated radar signatures for this optimum case are shown in Figure 5c.

Comparison with the observed radar signatures (Figure 5a) shows that only the NRCS profile for L band, HV, is reasonably reproduced in the simulation without wind variations. The simulated and observed NRCS profiles for VV and HH polarization are in poor agreement: The simulated NRCS profiles exhibit only an increase at the front, whereas the observed signatures show a more dip-like behavior. As already indicated, deviations between observed and simulated radar signatures at C band, HV polarization, may result from a poor SNR. The image acquired at C band, HV polarization, is therefore not included in our analysis. However, our model results for HH and VV polarization suggest that the observed multifrequency/multipolarization radar signatures cannot be sufficiently explained by pure current variations. This is a quite general conclusion, since the shapes of simulated radar signatures are not very sensitive to the choice of the equilibrium wave spectrum or other tunable elements of our model.

4.2. Variation of Atmospheric Parameters

Figure 5d shows results of a simulation run for a scenario which is supposed to resemble the wind forcing

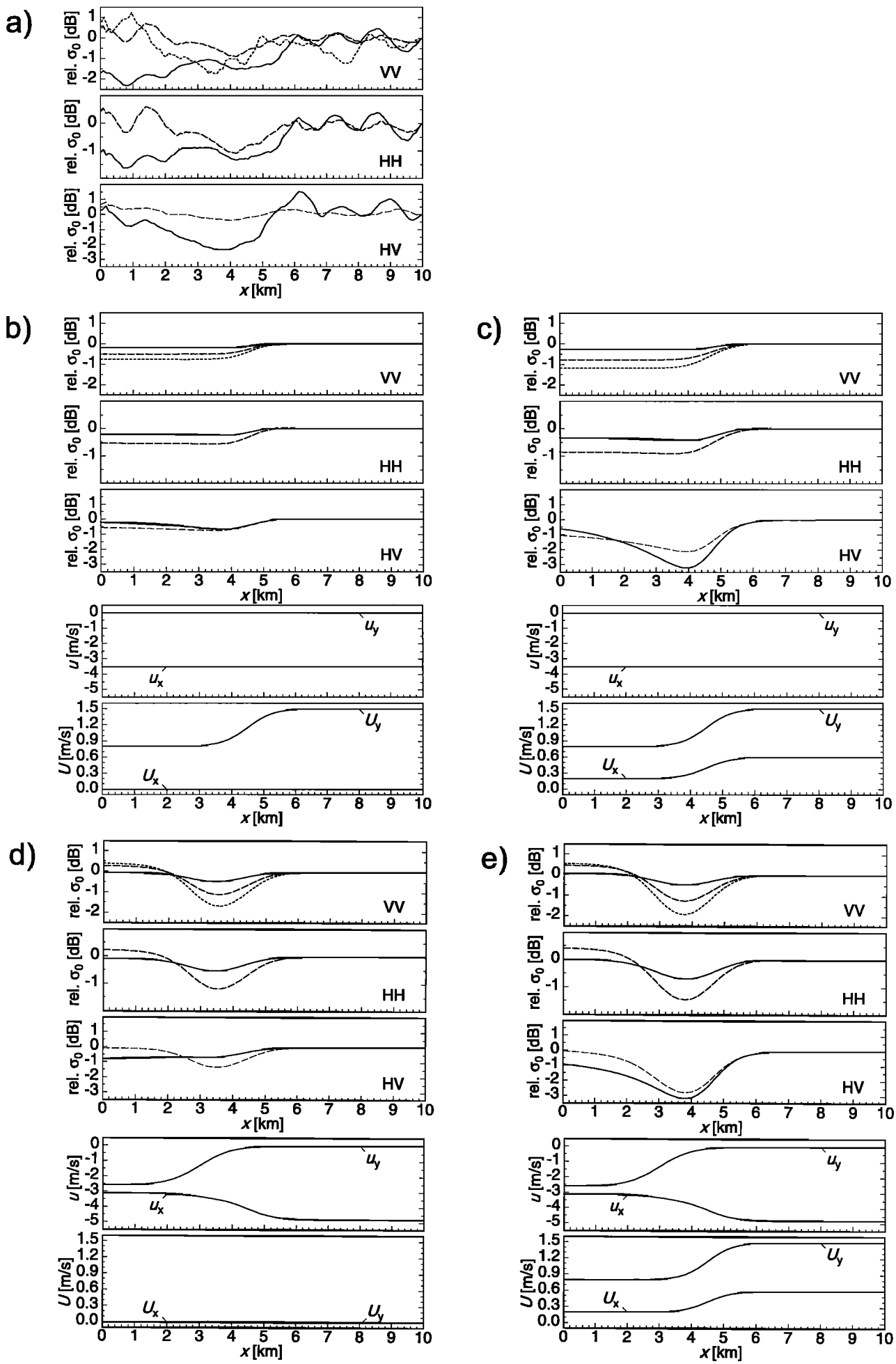
a)
b)
c)
d)
e)
rel. σ0 [dB]
VV
HH
HV
x [km]
u [m/s]
U [m/s]
uy
ux
Uy
Ux

conditions during the shuttle overflight without any currents. In the in situ data a sharp decrease of the wind speed from 9.0 $m\,s^{-1}$ (blowing from 90°N) to 3.5 $m\,s^{-1}$ (blowing from 130°N) was visible ~35 km before the front. Since the acquisition of these data was carried out ~2 hours before the shuttle overflight, it is very difficult to make detailed assumptions concerning the strength and position of this wind front at the time of the image acquisition. On the other hand, the radar images at almost all frequencies and polarizations show a bright, wedge-shaped region outside the Gulf Stream that enters the region of the intensity profiles of Figure 5. Thus we assume that an increase of NRCS values at this end of the profiles is due to an increase in wind speed, associated with a wind front like the one encountered in the in situ wind data. We have introduced a change of the actual wind vector $\boldsymbol{u}$ from the nominal value of 3.5 $m\,s^{-1}$ from 130°N to 4.0 $m\,s^{-1}$ from 90°N at the northwest end of the intensity profiles, 10 km before the front.

In addition to the explicit change of the wind vector the effect of thermal stratification of the MABL enters into the model assumptions in the way described in section 3, i.e., an increase of the effective wind speed from 3.5 to 4.8 $m\,s^{-1}$ above the Gulf Stream was assumed in order to account for the observed variation of the thermal stratification from stable to unstable and therefore the increase in wind stress.

The simulated wind-induced L band HV signature still shows a weak dip-like behavior but exhibits a much smaller modulation depth than the one from the current shear/divergence simulation. On the other hand, the observed radar signatures are reproduced quite well for C and X band at VV and HH polarization. Their profiles show a dip at the front that is similar to that of the observed NRCS profiles whereas the modulation depth has not changed significantly.

4.3. Combined Variation of Oceanic and Atmospheric Parameters

Finally, Figure 5e shows the results of a simulation run taking into account a combined current shear and divergence and the proposed variations in wind speed and atmospheric stratification. A comparison of Figure 5e with Figure 5a, which shows the measured NRCS variations, indicates that this scenario leads to best overall agreement between measured and simulated NRCS profiles.

In this context we would like to mention that all NRCS profiles in Figure 5 have been normalized by their values at $x = 10$ km in order to facilitate comparison of observed and simulated curves. The measured absolute NRCS values from SIR-C/X-SAR tend to be generally overestimated by our imaging model by amounts of ~2 dB at L band, ~3 dB at C band, and ~5 dB at X band. This effect is already known from other studies and does not indicate a fundamental problem of the proposed radar imaging theory. The equilibrium wave spectrum used in our simulations was optimized for the reproduction of reference NRCS values from airborne scatterometers, which have turned out to be systematically larger than NRCS values obtained from spaceborne SARs. However, equilibrium wave spectra proposed by different authors differ by as much as an order of magnitude in the Bragg wave region. As demonstrated by *Romeiser et al.* [1997], one can usually tune the wave spectrum within reasonable limits to adjust simulated NRCS levels by a few decibels. Such modifications would not affect shapes and modulation depths of simulated radar signatures very much. Accordingly, our findings regarding the specific dependencies of relative variations of the NRCS on current and wind variations and on radar parameters are quite general within the framework of the proposed model, despite the discrepancies between measured and simulated absolute NRCS values.

5. Discussion

The results of our investigations suggest that the observed radar signatures at the Gulf Stream front in Figure 1 are not caused by only one of the three factors: (1) current variation, (2) wind variation, or (3) change of the MABL stability. Instead, they are caused by a combination of these three factors. The fact that spatially varying surface currents and wind-forcing conditions modulate the ocean wave spectrum and thus the radar signatures at different frequencies and polarizations specifically allows the identification of oceanically and atmospherically induced signatures in the multifrequency/multipolarization radar imagery used in this study: According to our model results, radar signatures observed at HV polarization are mainly modulated by current variations, whereas the signatures at VV and HH polarization are essentially influenced by variations of the wind speed and thermal stratification. A discus-

Figure 5. Profiles of normalized radar backscattering cross section σ_0 at the Gulf Stream front, normalized by σ_0 at $x = 10$ km (top; dotted lines, X band; dashed lines, C band; solid lines, L band); (a) observed σ_0 profiles, obtained by averaging data over the width of the rectangular area marked in Figure 2. Results of a simulation run for (b) current shear and without current variation normal to the front at a constant wind vector; (c) optimized current shear and divergence at a constant wind vector; (d) no current but optimized wind forcing; (e) combined currents and winds from Figures 5c and 5d. Plots at bottom show model winds and currents for the respective cases.

sion on these differences between co polarization and cross polarization signatures of the Gulf Stream front is also given by *Chubb et al.* [1999].

Although the agreement between observed and simulated NRCS profiles is generally good for the proposed optimized parameter settings, a discrepancy remains between the measured and simulated curves for L band, VV and HH in the region outside the Gulf Stream: While the simulated NRCS shows a dip-like behavior at the front in all channels, the measured values at L band, VV and HH remain at a low level outside the Gulf Stream. This behavior may result from an approaching wind front which had reached the area just before the shuttle overflight. Under such conditions it is possible that the short ripple waves which act as resonant Bragg waves at X and C band had already picked up considerable amounts of energy, while the longer L band Bragg waves had not yet adjusted to the changing winds. One might think that the impact of rain on the ocean surface could be another explanation for the remaining discrepancy of the L band NRCS, but this possibility can be excluded as there was definitely no precipitation in the test area during the experiment.

Another point that requires critical consideration is the necessity of introducing a divergence at the Gulf Stream front to explain the observed radar signatures. Generally speaking, one would rather expect a convergence than a divergence coupled to the shear front, and there is no further evidence from the in situ data that would justify our result on the one hand. On the other hand, there is no in situ evidence for a convergence either, and in the course of a meandering structure like the Gulf Stream it is well possible to encounter frontal regions exhibiting a divergent flow due to ongoing movement or breakdown of the front. However, it seems that the introduced current divergence of 5.00×10^{-4} s^{-1} is fairly large compared to the current shear of 8.75×10^{-4} s^{-1}.

Finally, one should keep in mind that regardless of the fact that an advanced radar imaging model has been used for this study, our model results are still based on a number of simplifying assumptions. For example, it is not clear whether the actual effect of a spatially varying atmospheric stratification on the surface wave field is always adeqately represented by the effect of the proposed equivalent variations of u. Furthermore, our surface wave model does not yet account for effects like wave breaking [*Lyzenga,* 1996], feedback between surface roughness and wind stress [*Romeiser et al.,* 1994, 1999], or damping of waves in the presence of surface films [*Gade et al.,* 1998]. Inclusion of such effects may lead to significant changes in simulated radar signatures. Nevertheless, we believe that the main results of this study are quite robust and not very sensitive to future model modifications. Thus it appears that there is justification to drawing the following conclusions.

6. Conclusions

Observed multifrequency/multipolarization radar signatures of the Gulf Stream front have been compared with simulated radar signatures for different settings of oceanic and atmospheric parameters based on available in situ data. Special interest was laid on the specific characteristics of radar signatures resulting from surface current and wind stress variations and on the relative contributions of such signatures to the observed radar images at different frequencies and polarizations. It was found that the contributions of oceanic and atmospheric phenomena to radar signatures of the Gulf Stream front can be of comparable magnitude but exhibit different dependencies on radar frequency and polarization, which becomes particularly clear in the comparison of radar signatures at co polarization and cross polarization. On the basis of this knowledge, major characteristics of the observed multifrequency/multipolarization SIR-C/X-SAR radar signatures of the Gulf Stream front could be reproduced consistently by a numerical radar imaging model that accounts for the individual effects of current and wind stress variations. To our knowledge, comparable agreement between observed and simulated radar signatures of the Gulf Stream front at more than one frequency and polarization has never been achieved in previous studies that did not account for the combined effect of variations in the surface current and in the wind field.

The introduction of a fairly strong current divergence at the Gulf Stream front that is necessary to achieve optimum agreement of observed and simulated radar signatures across the front is a questionable element of our results which needs further investigation. The explanation of radar signatures of oceanic fronts is known to be a tough problem, and some new or improved theories of the radar imaging mechanism have been proposed just recently [e.g., *Lyzenga,* 1998]. A key problem is a lack of high-resolution current and wave data from oceanic fronts which are suited for a validation of such theories. This issue needs to be addressed in more detail in future projects and experiments. However, we think that one important and solid conclusion can be drawn from our results, despite some unresolved theoretical problems: Contributions of both hydrodynamic and aerodynamic modulation mechanisms must be taken into account for a realistic interpretation of radar signatures of oceanic fronts, and the combination of multifrequency/multipolarization radar images with a radar imaging model like the one used in this study allows to discriminate between these contributions and to estimate the strength of current and wind variations independently.

Acknowledgments. We would like to thank Tim Donato, Scott Chubb, and Farid Askari from NRL (Washington, D.C.) for providing in situ data and additional information for this study and our colleagues Martin Gade and

Werner Alpers for valuable discussions. This work has been supported by the European Commission, DG XII, as part of the Marine Science and Technology (MAST) program, contract MAS3-CT95-0035 (C-STAR), and by the German Space Agency (DARA) under contract 01QS9016/50QS90165 (X-SAR/SIR-C).

References

Alpers, W., Measurement of mesoscale oceanic and atmospheric phenomena by ERS-1 SAR, *Radio Sci. Bull., 275,* 14-22, 1995.

Askari, F., S. R. Chubb, T. Donato, W. Alpers, and S. A. Mango, Study of Gulf Stream features with a multifrequency polarimetric SAR from the space shuttle, in *Proceedings of the International Geoscience and Remote Sensing Symposium (IGARSS '97),* pp. 1521-1523, Inst. of Electr. and Electron. Eng., Piscataway, N. J., 1997.

Beal, R. C., V. N. Kudryavtsev, D. R. Thompson, S. A. Grodsky, D. G. Tilley, V. A. Dulov, and H. C. Graber, The influence of the marine atmospheric boundary layer on ERS 1 synthetic aperture radar imagery of the Gulf Stream, *J. Geophys. Res., 102,* 5799-5814, 1997.

Chubb, S. R., T. Donato, F. Askari, R. Romeiser, S. Ufermann, A.L. Cooper, W. Alpers, S. A. Mango, and J.-S. Lee, Study of Gulf Stream features with a multi-frequency polarimetric SAR from the Space Shuttle, *IEEE Trans. Geosci. Remote Sens.,* 2495-2507, 1999.

Gade, M., W. Alpers, S. A. Ermakov, and P. A. Lange, Wind-wave tank measurements of bound and freely propagating short gravity-capillary waves, *J. Geophys. Res., 103,* 21,697-21,709, 1998.

Jordan, R. L., B. L. Honeycutt, and M. Werner, The SIR-C/X-SAR synthetic aperture radar system, *IEEE Trans. Geosci. Remote Sens., 33,* 829-839, 1995.

Keller, W. C., V. Wismann, and W. Alpers, Tower-based measurements of the ocean C-band radar backscattering cross section, *J. Geophys. Res., 94,* 924-930, 1989.

Lyzenga, D. R., Effects of wave breaking on SAR signatures observed near the Gulf Stream, in *Proceedings of the International Geoscience and Remote Sensing Symposium (IGARSS '96),* pp. 908-910, Inst. of Electr. and Electron. Eng., Piscataway, N. J., 1996.

Lyzenga, D. R., Effects of intermediate-scale waves on radar signatures of ocean fronts and internal waves, *J. Geophys. Res., 103,* 18,759-18,768, 1998.

Mango, S. A., et al., Remote sensing of current-wave interaction with SIR-C/X-SAR during SRL-1 and SRL-2 at the Gulf Stream Supersite, in *Proceedings of the International Geoscience and Remote Sensing Symposium (IGARSS '95),* pp. 1325-1327, Inst. of Electr. and Electron. Eng., Piscataway, N. J., 1995.

Marmorino, G. O., R. W. Jansen, G. R. Valenzuela, C. L. Trump, J. S. Lee, and J. A. C. Kaiser, Gulf Stream surface convergence imaged by synthetic aperture radar, *J. Geophys. Res., 99,* 18,315-18,328, 1994.

Mitnik, L. M., Mesoscale coherent structures in the surface wind field during cold air outbreaks over the far eastern seas from the satellite side looking radar, *Mer, 30,* 297-314, 1992.

Romeiser, R., On the polarization-dependent signatures of atmospheric and oceanic features in radar images of the ocean surface, in *Proceedings of the International Geoscience and Remote Sensing Symposium (IGARSS '97),* pp. 1326-1328, Inst. of Electr. and Electron. Eng., Piscataway, N. J., 1997.

Romeiser, R., and W. Alpers, An improved composite surface model for the radar backscattering cross section of the ocean surface, 2, Model response to surface roughness variations and the radar imaging of underwater bottom topography, *J. Geophys. Res., 102,* 25,251-25,267, 1997.

Romeiser, R., A. Schmidt, and W. Alpers, A three-scale composite surface model for the ocean wave-radar modulation transfer function, *J. Geophys. Res., 99,* 9785-9801, 1994.

Romeiser, R., W. Alpers, and V. Wismann, An improved composite surface model for the radar backscattering cross section of the ocean surface, 1, Theory of the model and optimization/validation by scatterometer data, *J. Geophys. Res., 102,* 25,237-25,250, 1997.

Romeiser, R., S. Ufermann, and S. Stolte, Energy transfer between hydrodynamically modulated long and short ocean waves by interaction with the wind field, in *Proceedings of the International Geoscience and Remote Sensing Symposium (IGARSS '99),* pp. 965-967, Inst. of Electr. and Electron. Eng., Piscataway, N. J., 1999.

Rossby, T., The Gulf Stream: An introduction, *Maritimes, 35(1),* 1-2, 1991.

Tomczak, M., and J. S. Godfrey, *Regional Oceanography, An Introduction,* 422 pp., Pergamon, New York, 1994.

Ufermann, S., and R. Romeiser, Numerical study on signatures of atmospheric convective cells in radar images of the ocean, *J. Geophys. Res.,* this issue.

Ufermann, S., M. Gade, R. Romeiser, and W. Alpers, On the impact of lower atmospheric stratification on SAR images of the ocean surface, in *Operational Remote Sensing for Sustainable Development,* edited by G. A. Nieuwenhuis, R. A. Vaughan, and M. Molenaar, pp. 261-265, Balkema, Rotterdam, 1999.

Valenzuela, G. R., Theories for the interaction of electromagnetic and ocean waves—A review, *Boundary Layer Meteorol., 13,* 61-85, 1978.

Valenzuela, G. R., R. P. Mied, A. R. Ochadlick, M. Kobrick, P. M. Smith, F. Askari, R. J. Lai, D. Sheres, J. M. Morrison, and R. C. Beal, The July 1990 Gulf Stream Experiment, in *Proceedings of the International Geoscience and Remote Sensing Symposium (IGARSS '91),* pp. 119-122, Inst. of Electr. and Electron. Eng., Piscataway, N. J., 1991.

Valenzuela, G. R., S. R. Chubb, S. A. Mango, F. Askari, B. Holt, W. Alpers, T. Donato, and E. H. H. Shih, Remote sensing of current-wave interaction with SIR-C/X-SAR (SRL-1) at the Gulf Stream Supersite, in *Proceedings of the International Geoscience and Remote Sensing Symposium (IGARSS '94),* pp. 1728-1731, Inst. of Electr. and Electron. Eng., Piscataway, N. J., 1994.

Wright, J. W., A new model for sea clutter, *IEEE Trans. Antennas Propag., AP-16,* 217-223, 1968.

Wu, J., Effects of atmospheric stability on ocean ripples: A comparison between optical and microwave measurements, *J. Geophys. Res., 96,* 7265-7269, 1991.

Zink, M., and R. Bamler, X-SAR radiometric calibration and data quality, *IEEE Trans. Geosci. Remote Sens., 33,* 840-847, 1995.

R. Romeiser, Institute of Oceanography, University of Hamburg, Troplowitzstraße 7, 22529 Hamburg, Germany. (romeiser@ifm.uni-hamburg.de)

S. Ufermann, Southampton Oceanography Centre, School of Ocean and Earth Science, European Way, Southampton, SO14 3ZH, United Kingdom. (ufermann@soton.ac.uk)

(Received October 7, 1998; revised July 13, 1999; accepted August 10, 1999.)